

Adaptive Internal Models: Explaining the Oculomotor System and the Cerebellum

Mireille E. Broucke

Department of Electrical and Computer Engineering

University of Toronto

February 9, 2021

1. INTRODUCTION

This report presents a control-theoretic model of the oculomotor system, particularly the vestibulo-ocular reflex, gaze fixation, and the smooth pursuit system, and including the interactions between the brainstem and the cerebellum. Parts of this report have been published in an IFAC conference paper [9] and as an IEEE TAC paper [10].

We show that developments on adaptive internal models [49,56,65,66] provide a compelling framework to explain this system. We obtain a model that is simple yet is able to explain more behaviors than previously proposed models. In addition, we make a proposal about the function of the cerebellum. A computational model of the cerebellum is one of the great open problems of neuroscience today. Our model suggests that the cerebellum embodies adaptive internal models of persistent, exogenous disturbance and reference signals observable through the error signals arriving at the cerebellum.

Control theory has been well accepted as a mathematical basis to explain motor control systems for many decades. A number of unified control-theoretic models of the oculomotor system, in particular, have been proposed in [28,58,64,80,81,84], among others. However, these models are limited in the behaviors they capture, and further, certain behaviors such as the so-called predictive capability of the smooth pursuit system have not yet been fully characterized. Meanwhile, since the 1990's neuroscientists have explored internal models as a means to explain the function of the cerebellum. And there is mounting interest in the control community, as witnessed by a session on internal models in neuroscience in the 2018 IEEE Conference on Decision and Control. Despite mounting interest in both communities, a computational model of the cerebellum that includes the internal model principle has never been formalized, to date. In sum, to the best of our knowledge, we present here the first control theoretic model of the oculomotor system and the cerebellum that incorporates the internal model principle of control theory [23,24].

The oculomotor system comprises several eye movement systems: the *vestibulo-ocular reflex* (VOR), *optokinetic reflex* (OKR), the *saccadic system*, the *gaze fixation system*, the *smooth pursuit system*, and the *vergence system*. The VOR serves to keep the gaze (sum of eye and head angles) stationary when the head is moving. The OKR reduces image motion across the retina when a large object or the entire visual surround is moving. The saccadic system provides rapid, discrete changes of eye position in order to place an object of interest on the fovea. The gaze fixation system stabilizes the gaze on a stationary object. The smooth pursuit system keeps a moving object centered on the fovea. The vergence system coordinates the movement of the two eyes.

The oculomotor system anatomy includes the oculomotor plant consisting of the eyeball, muscles moving the eye, and oculomotor neurons that stimulate the muscles; the brainstem which provides the main feedback loop by receiving the retinal and vestibular (from the semicircular canals of the ear) signals and issuing the oculomotor command to the eye muscles; and the cerebellum which regulates eye movements as a top up to the main control loop through the brainstem.

The cerebellum is a purely feedforward, uniform, laminated brain structure that is divided into functional zones; e.g. locomotion, posture control, eye movement, arm movement, speech regulation, etc. Our concern here is with the vestibulocerebellum or floccular complex, which is responsible for regulating eye movements. Each cerebellar zone receives two types of inputs on *mossy fibers* and *climbing fibers*. The sole output of the cerebellum is through the *Purkinje cells* of the cerebellar cortex. The *cerebellar microcircuit*, consisting of Purkinje cells, basket cells, Gogli cells, granule cells, stellate cells, mossy fibers, climbing fibers, and parallel fibers, has been fully characterized [25].

This report focuses on the VOR, gaze holding, and smooth pursuit. For simplicity we consider only horizontal movement of a single eye; other aspects not covered by our model are discussed in Section 5. Next we highlight features of our model in addition to our use of the internal model principle.

Error Signals. Each of the eye movement systems has driving signals, signals required for computation of ongoing eye movement. Head velocity is a driving signal for the VOR. *Retinal error*, the difference between the target and fovea positions on the retina, drives the saccadic system [58]. *Retinal slip velocity*, the time derivative of retinal error, is often assumed to be the driving signal for the smooth pursuit system (despite the mathematical dilemma of how positional errors can be driven to zero using only velocity errors). It is known that in primates, the VOR, gaze holding, and smooth pursuit systems share the same neural pathways in the brainstem and cerebellum¹, so it is plausible these systems share certain driving signals [13, 45]. We assume that a common visual driving signal shared by the VOR, gaze holding, and smooth pursuit systems is the retinal error. This signal is believed to arise in the superior colliculus of the brainstem [6, 28, 38, 39].

Evidence for the relevance of retinal error as a driving signal of the VOR, gaze holding, and smooth pursuit is reported in [7, 21, 67, 68, 85]. A series of studies by Pola and Wyatt [59, 76, 77] showed that retinal slip velocity is inadequate to explain all the behaviors of the smooth pursuit system. Other studies used strobe-reared cats, who never experience retinal slip velocity [48, 50]. Finally, direct experimental evidence that retinal errors drive the smooth pursuit system was given in [8]; they used a flashing visual target for which no velocity information could be perceived directly.

Brainstem v.s. Cerebellum. There has been considerable research both to understand how the VOR, OKR, gaze holding, and smooth pursuit systems interact, as well as to differentiate which computations arise in the cerebellum versus the brainstem. For the VOR, several authors have proposed that there is a switching or gating mechanism that chooses between vestibular (head movement) and retinal error signals [11, 41].

In our model, the control input generated in the brainstem-only pathway is a linear combination of eye movement information and vestibular inputs. Specifically, we assume the brainstem cancels a part of the vestibular signal (to generate the VOR) and a part of the disturbance introduced by the oculomotor plant itself. Instead, the cerebellum receives only visual information. Its role is to provide a top up to the disturbance suppression activities of the brainstem. This view is consistent with the *flocculus central vestibular neuron complementary hypothesis* of [13]. It postulates that the cerebellum will be modulated if the signal provided by central vestibular neurons (the brainstem) is not sufficient to achieve the objectives of the VOR, OKR, or smooth pursuit.

Finally, we assume that when the visual driving signal is removed, as in darkness, the cerebellum falls inactive. Numerous studies support the idea that the cerebellum (the flocculus) is relatively inactive without visual input [45]. This interpretation is corroborated by experiments in which a sudden change in oculomotor behavior known to be mediated by the cerebellum occurs when the lights are turned on.

Corollary Discharge. A long-standing debate in the neuroscience community regards how eye position information becomes available to the brain. One theory dating to the 1800's proposed that the brain receives an *effference copy* of an internal signal carrying eye position information. An opposing theory argues that *proprioception* of eye muscle activity provides eye movement information, obviating the need for effference copies. In the 1950's, the term *corollary discharge* was coined to characterize a copy of the motor command that informs the brain of ongoing eye movement.

It has been proven experimentally that proprioception from the eye muscles plays a negligible role in eye movement [15, 32, 37]. Consonant with these findings, our model assumes no proprioception. The *brainstem neural integrator* is now regarded to be the mechanism that provides the eye position to the brainstem [58]. In this work, we write the neural integrator in the form of an observer of the oculomotor plant. Our observer equation is identical to a leaky integrator in the Laplace domain, therefore matching experimental findings [69].

Since in our model the cerebellum only receives visual information, ongoing eye movement information is not directly supplied to the cerebellum. Our proposal is that residing in the cerebellum is an internal model of all exogenous disturbances acting on the oculomotor system and observable through the retinal

¹When we use the term *cerebellum*, we refer more specifically to the floccular complex, comprising the flocculus and the ventral paraflocculus [44].

error signal. The states of the internal model provide the signals for ongoing activity of the eye in the cerebellum, even with zero retinal slip. In our model, such extraretinal signals arise in the cerebellum by using a corollary discharge of the motor command.

Internal Models. Theories on the function of the cerebellum have been dominated by internal models for at least 25 years [29, 34, 35, 51, 73–75]. One view is that the cerebellum provides a *forward model* of the system to be controlled [34, 51]. Another theory called *feedback error learning* (FEL) argues the cerebellum provides *inverse models* [29, 35]. Another is that multiple forward and inverse models reside in the cerebellum [74]. These theories are related to notions in robotics on forward and inverse kinematics; indeed FEL is a variant of the computed torque method in robotics. We notice the term “internal model” in the neuroscience literature is distinct from the internal model principle of control theory [23, 24].

It seems reasonable that the brain would require kinematic models of the body, both as forward and inverse models. But we do not relegate this role to the cerebellum. Rather, our work here mathematically formalizes the idea that the role of the cerebellum is to realize the internal model principle: *to provide internal models of persistent, exogenous signals acting on a biological system.*

The idea that the cerebellum or other regions of the brain may be involved in generating internal models of exogenous signals has already been suggested [16, 17, 44]. Particularly, in the review article [44], Lisberger presents three theories about the type of internal model that may reside in the cerebellum to support the oculomotor system. His first theory is that the cerebellum provides a model of the inertia of realworld objects - we can interpret his statement as an instance of the internal model principle.

Experimental evidence from the oculomotor system for the existence of internal models of exogenous signals comes in four forms. First, there is the so-called predictive capability of the smooth pursuit system - to track moving targets with zero steady-state error [2, 20, 79]. Second, it has been shown experimentally that exogenous signals that can be modeled by low-order linear exosystems are easily tracked, while unpredictable signals are not [3, 18, 20, 52]. Third, in an experiment called *target blanking*, a moving target is temporarily occluded, yet the eye continues to move [16, 17]; researchers postulate the brain has an internal model of the motion of the target. The fourth evidence comes from an experiment called the *error clamp*, in which the retinal error is artificially clamped at zero using an experimental apparatus that places the target image on the fovea [5, 55, 70]. Despite zero retinal error, the eye continues to track the target, suggesting that extraretinal signals drive the pursuit system.

Organization. This report is organized as follows. In the next section we derive the open-loop model of the oculomotor system. In Section 3 we derive the error model, formulate the disturbance rejection problem, and solve the problem using the theory of adaptive internal models. In Section 4 we present simulation results. In Section 5 we compare our model architecture to current architectures involving the cerebellum. Concluding remarks are presented in Section 6.

2. OPEN-LOOP MODEL

The horizontal motion of the eye is modeled by considering the eyeball as a sphere that is suspended in fluid and subjected to viscous drag, elastic restoring forces, and the pulling of two muscles [63, 71]. A reasonable approximation is obtained by assuming that the inertia of the eyeball is insignificant. Letting x be the horizontal eye angle and u be the net torque imparted by the two muscles, we obtain a first order model

$$\dot{x} = -K_x x + u. \quad (1)$$

The parameter $K_x > 0$ is constant (or very slowly varying) such that the time constant of the eye is $\tau_x := 1/K_x \simeq 0.2\text{s}$ [63]. This first order model may be compared with the model of an ocular motoneuron. Let f be the firing rate, and let f_0 be the baseline firing rate when the eye is stationary at $x = 0$. A commonly used model of neuronal firing rate is $f = f_0 + c_1 x + c_2 \dot{x}$, where c_1 and $c_2 \neq 0$ are constants [61, 63, 71]. Comparing this model with (1), we observe that $K_x = c_1/c_2$ and $u = \frac{1}{c_2}(f - f_0)$. That is, the torque is proportional to the firing rate, modulo a constant offset of f_0 .

Next consider a reference signal r representing the angle of a target moving in the horizontal plane. Let x_h and \dot{x}_h be the horizontal head angular position and angular velocity, respectively. The *retinal error* is

defined to be

$$e := \alpha_e(r - x_h - x). \quad (2)$$

Notice that $r - x_h - x$ is the target angle r relative to the *gaze angle* $x_h + x$. For sufficiently distant targets, this relative angle is proportional (through the scale factor $\alpha_e \in \mathbb{R}$) to a linear displacement on the retina from the fovea to the target. Since the goal of the VOR, OKR, gaze holding, and smooth pursuit is to drive e to zero, for the purposes of the present paper we set $\alpha_e = 1$, since for $\alpha_e \neq 1$ we can always redefine the error to be $e' = e/\alpha_e$.

We assume that the control input u takes the form

$$u = u_b + u_c,$$

where the brainstem component u_b is generated through a brainstem-only pathway, while the cerebellar component u_c is generated by a side pathway through the cerebellum. The reference signal r is treated as a persistent unmeasurable disturbance acting on the oculomotor system. The eye position x is assumed to be unavailable for direct measurement [15, 32, 37]. The vestibular system provides a measurement of the head angular velocity \dot{x}_h to the brainstem but not directly to the cerebellum [27, 63], and it does not provide the head position x_h [63]. Finally, we assume that both the brainstem and the cerebellum receive a measurement of the retinal error e (or a scaled version of it) based on retinal information supplied by a brain region such as the superior colliculus [6, 28, 39].

Because we assume the retinal error is available for measurement, it is unnecessary to have measurements of x or x_h since, in theory, these signals can be reconstructed based on observability through e . In practice, the phylogenetically older brainstem likely evolved without the benefits of observability; therefore, it receives certain measurements (such as \dot{x}_h) directly. Moreover, there is reason to believe a brainstem-only pathway serves the VOR to cancel voluntary head movements, while the cerebellum serves to cancel exogenous, involuntary head movements and target motion.

To model the brainstem, we start from Robinson's parallel pathway model [69] consisting of two parallel pathways that combine to form the motor command; that is, $u = u_v + u_n$, where u_v is carried on the direct pathway, and u_n corresponds to the indirect pathway. The signal u_n is the output of the *brainstem neural integrator* [69]. Invoking equation (3) in [62], the neural integrator is modeled as a leaky integrator:

$$\dot{\hat{x}} = -\tilde{K}_x \hat{x} + u_v, \quad u_n = \alpha_x \hat{x}, \quad (3)$$

where α_x and \tilde{K}_x are constants (or very slowly varying). Using the fact that $u_v = u - \alpha_x \hat{x}$, this model can be re-expressed as

$$\dot{\hat{x}} = -\hat{K}_x \hat{x} + u, \quad (4)$$

where $\hat{K}_x := \tilde{K}_x + \alpha_x$. Finally, we incorporate the idea from [26] that $\hat{K}_x \simeq K_x$ (henceforth we drop the hat); see also [19, 30]. In sum, we deduce that the brainstem neural integrator forms an *observer* of the oculomotor plant. If we define the estimation error $\tilde{x} := x - \hat{x}$, then \tilde{x} evolves according to $\dot{\tilde{x}} = -K_x \tilde{x}$, implying that $\hat{x}(t)$ converges exponentially to $x(t)$. Aside from a momentary perturbation (a push on the eyeball), $\hat{x}(t)$ well approximates $x(t)$.

Remark 2.1. The neural integrator contributes to a distributed gaze holding function, resulting in three time constants for gaze holding: $\tau_x = 0.2\text{s}$ is the time constant of the oculomotor plant; $\tilde{\tau}_x = 1/\tilde{K}_x = 2\text{s}$ is the time constant of the combined neural integrator and plant; and the time constant induced by the top up from the cerebellum is $\tau = 25\text{s}$ [28]. \triangleleft

To complete the modeling of the brainstem, we consider the components of the signal u_v . In our model $u_v = u_c - \alpha_h \dot{x}_h$, where u_c contains visual information and the output of the cerebellum, and $\alpha_h \dot{x}_h$ is the vestibular measurement of head angular velocity representing the direct feedthrough from the semicircular canals to the oculomotor plant. The overall motor command is

$$u = u_v + u_n = \alpha_x \hat{x} - \alpha_h \dot{x}_h + u_c,$$

so the brainstem-only pathway of the control input is

$$u_b = \alpha_x \hat{x} - \alpha_h \dot{x}_h, \quad (5)$$

where $\alpha_x \in \mathbb{R}$ and $\alpha_h \in \mathbb{R}$ are constant (or slowly varying) parameters; and once again, \dot{x}_h is the head angular velocity, and \hat{x} is an estimate of the eye position. We can see that the role of u_b is to suppress a portion of the head velocity disturbance and to partially cancel the drift term in the oculomotor plant dynamics.

3. DISTURBANCE REJECTION PROBLEM

We approach the derivation of a model of the cerebellum as a problem of control synthesis: to design a controller u_c to drive the error $e(t)$ to zero. Assuming that $\hat{x}(t) \simeq x(t)$ for $t \geq 0$, we obtain the *error model*

$$\dot{e} = -\tilde{K}_x e - u_c + \dot{r} + \tilde{K}_x r - (1 - \alpha_h)\dot{x}_h - \tilde{K}_x x_h, \quad (6)$$

where $\tilde{K}_x = K_x - \alpha_x$. We assume that the reference signal r as well as the head position x_h are modeled as the outputs of a linear exosystem. Let $\eta \in \mathbb{R}^q$ be the exosystem state and define the exosystem

$$\dot{\eta} = S\eta \quad (7a)$$

$$r = D_1\eta, \quad x_h = D_2\eta, \quad (7b)$$

where $S \in \mathbb{R}^{q \times q}$, $D_1 \in \mathbb{R}^{1 \times q}$, and $D_2 \in \mathbb{R}^{1 \times q}$. Then (6) takes the form

$$\dot{e} = -\tilde{K}_x e - u_c + E\eta \quad (8)$$

where $E := D_1 S + \tilde{K}_x D_1 - (1 - \alpha_h)D_2 S - \tilde{K}_x D_2 \in \mathbb{R}^{1 \times q}$.

It is useful to transform the exosystem using the technique in [56]. Let (F, G) be a controllable pair with F Hurwitz. Specifically, we take

$$F = \begin{bmatrix} 0 & 1 & \cdots & 0 & 0 \\ \vdots & & & \ddots & \\ 0 & 0 & \cdots & 0 & 1 \\ -\lambda_1 & -\lambda_2 & \cdots & & -\lambda_q \end{bmatrix}, \quad G = \begin{bmatrix} 0 \\ \vdots \\ 0 \\ 1 \end{bmatrix}, \quad (9)$$

where the polynomial $s^q + \lambda_q s^{q-1} + \cdots + \lambda_1$ is Hurwitz. Define the coordinate transformation $w = M\eta$, with $M \in \mathbb{R}^{q \times q}$ nonsingular and satisfying the Sylvester equation $MS = FM + GE$ (without loss of generality we can assume (E, S) is observable and the spectra of S and F are disjoint) [56]. Also define $\Psi := EM^{-1} \in \mathbb{R}^{1 \times q}$. In new coordinates, the exosystem model is

$$\dot{w} = (F + G\Psi)w. \quad (10)$$

Because $E\eta = \Psi w$, we can write the error dynamics (8) in terms of the new exosystem state:

$$\dot{e} = -\tilde{K}_x e - u_c + \Psi w. \quad (11)$$

The parameters $(\tilde{K}_x, \Psi^T) \in \mathbb{R}^{q+1}$ capture all unknown model and disturbance parameters.

Problem 3.1. Consider the error dynamics (11). Suppose the unknown parameters (\tilde{K}_x, Ψ^T) belong to a known compact set $\mathcal{P} \subset \mathbb{R}^{q+1}$. We want to find an error feedback controller

$$\begin{aligned} \dot{\xi} &= F_c(\xi, e) \\ u_c &= H_c \xi + K_c e \end{aligned}$$

such that for all initial conditions $(e(0), w(0), \xi(0))$ and for all $(\tilde{K}_x, \Psi^T) \in \mathcal{P}$, the solution $(e(t), w(t), \xi(t))$ of the closed loop system

$$\begin{aligned} \dot{e} &= -(\tilde{K}_x + K_c)e - H_c \xi + \Psi w \\ \dot{\xi} &= F_c(\xi, e) \end{aligned}$$

satisfies $\lim_{t \rightarrow \infty} e(t) = 0$.

We invoke the design approach of [65, 66]. The controller takes the form of an *adaptive internal model* consisting of an internal model of the disturbances acting on the oculomotor system combined with a parameter estimation process to recover the unknown parameters. Let \hat{w} and $\hat{\Psi}$ be estimates of w and Ψ , respectively. The controller is

$$\dot{\hat{w}} = F\hat{w} + Gu_c \quad (12)$$

$$u_c = u_{imp} + u_s. \quad (13)$$

The controller u_{imp} is selected to satisfy the internal model principle: $u_{imp} = \hat{\Psi}\hat{w}$. The controller u_s is selected to make the closed-loop system asymptotically stable. We choose $u_s = K_e e$, with $K_e > 0$ sufficiently large. Based on a Lyapunov argument, the adaptation law for the parameter estimates is $\dot{\hat{\Psi}} = e\hat{w}^T$.

In summary, the overall model is

$$\dot{\hat{x}} = -K_x \hat{x} + u \quad (14a)$$

$$\dot{\hat{w}} = F\hat{w} + Gu_c \quad (14b)$$

$$\dot{\hat{\Psi}} = e\hat{w}^T \quad (14c)$$

$$u_b = \alpha_x \hat{x} - \alpha_h \dot{x}_h \quad (14d)$$

$$u_c = \hat{\Psi}\hat{w} + K_e e \quad (14e)$$

$$u = u_b + u_c. \quad (14f)$$

A proof of correctness of this design is provided in the Appendix.

4. SIMULATION RESULTS

In this section we simulate our model under a number of experimental scenarios involving the VOR, OKR, gaze holding, and smooth pursuit. The parameter values for the simulations are: $q = 2$, $K_x = 5$, $\alpha_x = 0.95K_x$, $\alpha_h = 0.65$, $K_e = 5$, $\lambda_1 = 1$, and $\lambda_2 = 1$. In a few cases noted below, different parameters are used to exaggerate certain transient phenomena.

4.1. VOR. We consider the VOR in which the eye must track a fixed target while the head is moving. First, we consider what happens when the head is rotated in darkness. It is known that the cerebellum is relatively inactive due to a lack of visual input [45]. As such, we assume in darkness $u_c = 0$, so the eye dynamics evolve according to a brainstem-only control input. Assuming that $x(t) \simeq \hat{x}(t)$, we have

$$\dot{x} = -\tilde{K}_x x - \alpha_h \dot{x}_h. \quad (15)$$

Suppose $x_h(t) = a_h \sin(\beta_h t)$, and let Ω be the limit set of any solution of (15). Assuming $\tilde{K}_x > 0$, a solution $x_\infty(t)$ in Ω has the form

$$x_\infty(t) = -\alpha_h a_h \frac{\beta_h}{\tilde{K}_x^2 + \beta_h^2} \left(\beta_h \sin(\beta_h t) - \tilde{K}_x \cos(\beta_h t) \right).$$

Generally $\tilde{K}_x \ll \beta_h$, so

$$x_\infty(t) \simeq -\alpha_h a_h \sin(\beta_h t) = -\alpha_h x_h(t).$$

That is, the eye moves relative to the head with a scale factor of $-\alpha_h$. The parameter α_h is called the *VOR gain* since it well approximates the ratio of head velocity to eye velocity measured in darkness. We note that our model predicts that the VOR in the dark is unaffected by disabling the cerebellum, as reported experimentally [63, 83].

The standard VOR experiment is to apply an involuntary sinusoidal head rotation: $x_h(t) = a_h \sin(\beta_h t)$, where $a_h, \beta_h > 0$. Figure 1 shows simulation results for the values $a_h = 15$, $\beta_h = 0.1\text{Hz}$ for $t \in [0, 10]$, and $\beta_h = 0.2\text{Hz}$ for $t \in [10, 20]$. The initial condition on all states is zero except the eye angle, which starts at $x(0) = -10^\circ$. We also plot the retinal error e , the cerebellar output u_{imp} , the brainstem component u_b , and the parameter estimates $\hat{\Psi}_1$ and $\hat{\Psi}_2$. As expected, the eye moves opposite to the head rotation, and it adapts to the frequency of the sinusoidal disturbance.

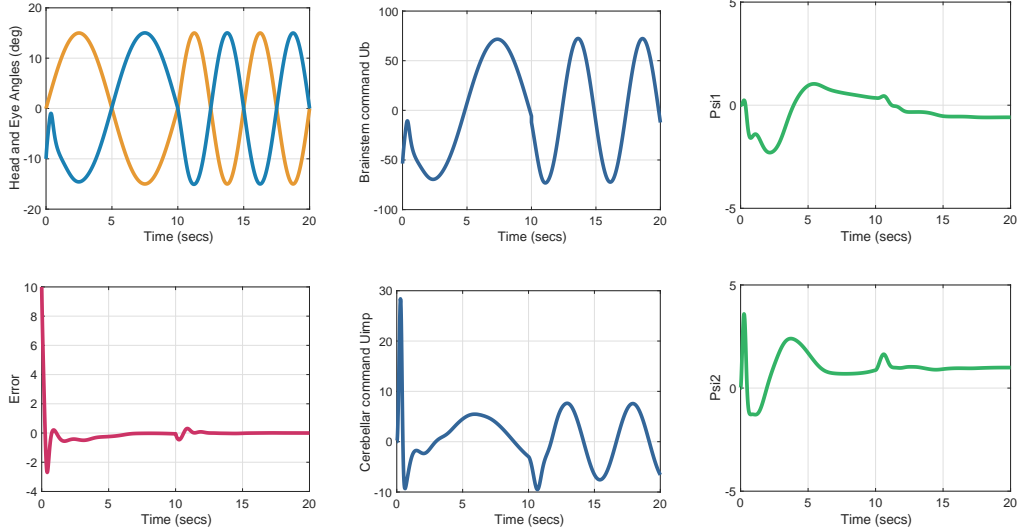


FIGURE 1. VOR with a sinusoidal head rotation. The top left figure shows the head (yellow) and eye (blue) angles. The bottom left is the retinal error (red). The middle figures are u_b and u_{imp} , and the right figures are the parameter estimates $\hat{\Psi}_1$ and $\hat{\Psi}_2$.

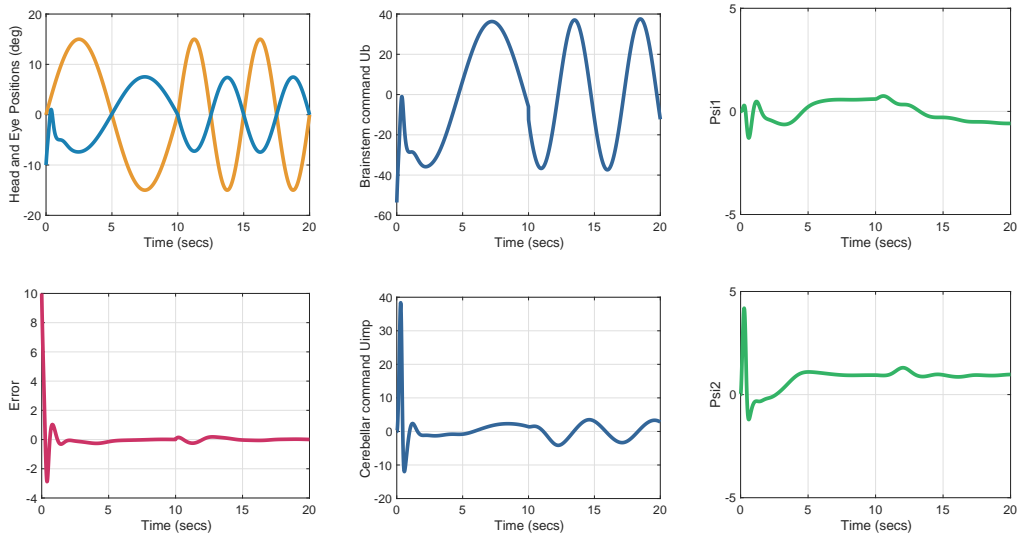


FIGURE 2. VOR while tracking a target moving relative to the head rotation. The top left figure shows the head (yellow) and eye (blue) angles. The bottom left is the retinal error (red). The middle figures are u_b and u_{imp} , and the right figures are the parameter estimates $\hat{\Psi}_1$ and $\hat{\Psi}_2$.

A second standard experiment is to evoke *short-term adaptation* of the VOR. For example, suppose an involuntary sinusoidal head rotation is applied $x_h(t) = a_h \sin(\beta_h t)$, where $a_h, \beta_h > 0$, while at the same time the subject must track a target $r(t) = \alpha_r x_h(t)$, where α_r is a constant. Figure 2 shows simulation results for $\alpha_r = 0.5$, $a_h = 15$, $\beta_h = 0.1\text{Hz}$ for $t \in [0, 10]$, and $\beta_h = 0.2\text{Hz}$ for $t \in [10, 20]$. The initial condition on all states is zero except the eye angle, which starts at $x(0) = -10^\circ$. We also plot the retinal error e , the cerebellar output u_{imp} , the brainstem component u_b , and the parameter estimates $\hat{\Psi}_1$ and $\hat{\Psi}_2$. The eye moves opposite to the head rotation, but only with half the amplitude.

An experiment reported in [46] demonstrated that the depth of firing rate of the output of the cerebellum, u_{imp} in our model, increases with the frequency of head rotation. This behavior is predicted by our model

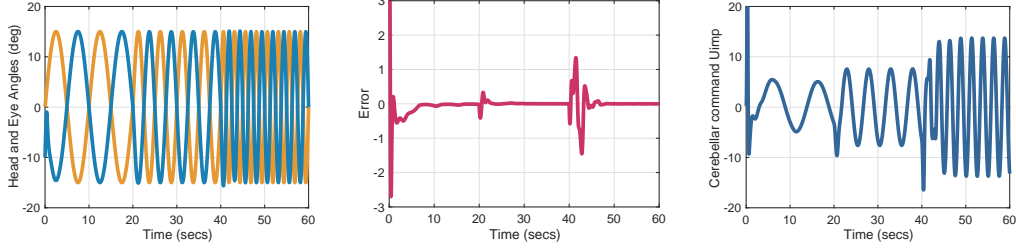


FIGURE 3. Effect of the frequency of oscillations of the head on the depth of modulation of the cerebellar output u_{imp} . From left to right, the head (yellow) and eye (blue) angles, the retinal error e , and the cerebellar output u_{imp} .

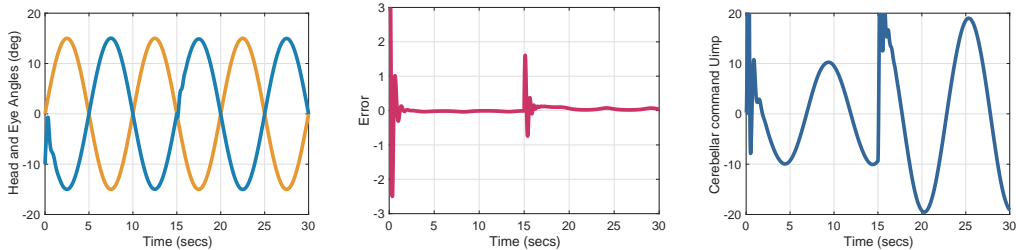


FIGURE 4. Effect of α_h on the VOR. From left to right, the head (yellow) and eye (blue) angles, the retinal error e , and the cerebellar output u_{imp} .

because $u_{imp} = \hat{\Psi}\hat{w}$ must build an estimate of $-(1-\alpha_h)\dot{x}_h - \tilde{K}_x x_h$. In particular, the term $\dot{x}_h = a_h \beta_h \cos(\beta_h t)$ is proportional to β_h . This behavior is depicted in Figure 3 by simulating our model with the values $a_h = 15$, $\beta_h = 0.1\text{Hz}$ for $t \in [0, 20]$, $\beta_h = 0.2\text{Hz}$ for $t \in [20, 40]$, and $\beta_h = 0.5\text{Hz}$ for $t \in [40, 60]$. We see in the right figure of Figure 3 that the amplitude of u_{imp} increases as the frequency of the head rotation increases.

It has been demonstrated that the VOR in the light is unaffected by changes in the VOR gain [53]. Figure 4 shows this experimental behavior with our model, where $\alpha_h = 2$ for $t \in [0, 15]$ and $\alpha_h = -1$ for $t \in [15, 30]$. It is clear from the left figure that our model predicts that in steady-state, the VOR in the light is unaffected by changes in the VOR gain.

An experiment investigating the transients of the VOR in monkeys was reported in [47]. It was discovered that the overshoot in the eye velocity to a sudden rotation of the head was larger when the VOR gain is smaller. In the experiment, a light spot at $r = 0$ on which the monkey fixates (in another otherwise dark room) is strobed. Here we assume the subject attempts to continuously fixate the eyes on a target at $r = 0$, even when the light spot is extinguished. The head position is a ramp function: $x_h(t) = 0$ for $t \in [0, 1]$ and $x_h(t) = -30t$ for $t \in [1, 5]$, resulting in a head angular velocity of $-30^\circ/\text{s}$. Figure 5 illustrates that our model recovers the behavior in [47]. The blue curve is the eye angular velocity for $\alpha_h = 0.3$, red is with $\alpha_h = 0.5$, and yellow is with $\alpha_h = 0.8$. We see clearly that smaller VOR gains result in larger overshoots.

In an experiment called *VOR cancellation*, the head is rotated involuntarily while the eyes must track a head-fixed target [13]. Suppose the head angle is $x_h(t) = a_h \sin(\beta_h t)$ with $a_h, \beta_h > 0$, and the target angle is $r(t) = x_h(t)$. Then the error is given by $e = -x$. The role of u_{imp} in this case is to cancel the disturbance $\alpha_h \dot{x}_h$ introduced by the brainstem component u_b . Figure 6 illustrates the results for VOR cancellation using our model. Particularly, we note that the response amplitude of the brainstem component is not reduced during VOR cancellation, as experimentally confirmed in [12, 36].

A number of researchers have studied the VOR in the situation when the cerebellum is disabled either due to disease or cerebellectomy [15, 82, 83]. We illustrate this effect for the previous scenario of VOR cancellation, but now with $u_c = 0$. Simulation results are shown in Figure 7. What we observe in the left figure is that the subject is no longer able to suppress the VOR - the blue curve shows that the eye position is not stabilized, despite a head-fixed target. This result corroborates the experimental findings in [83].

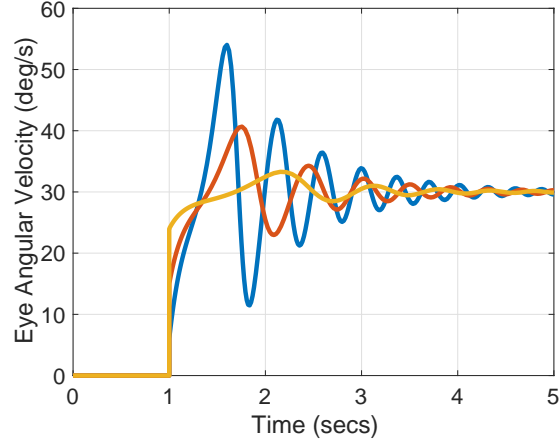


FIGURE 5. VOR with a step input in head velocity for the values $\alpha_h = 0.3, 0.5, 0.8$ (blue, red, yellow). The size of the overshoot in the eye velocity is inversely proportional to the value of α_h .

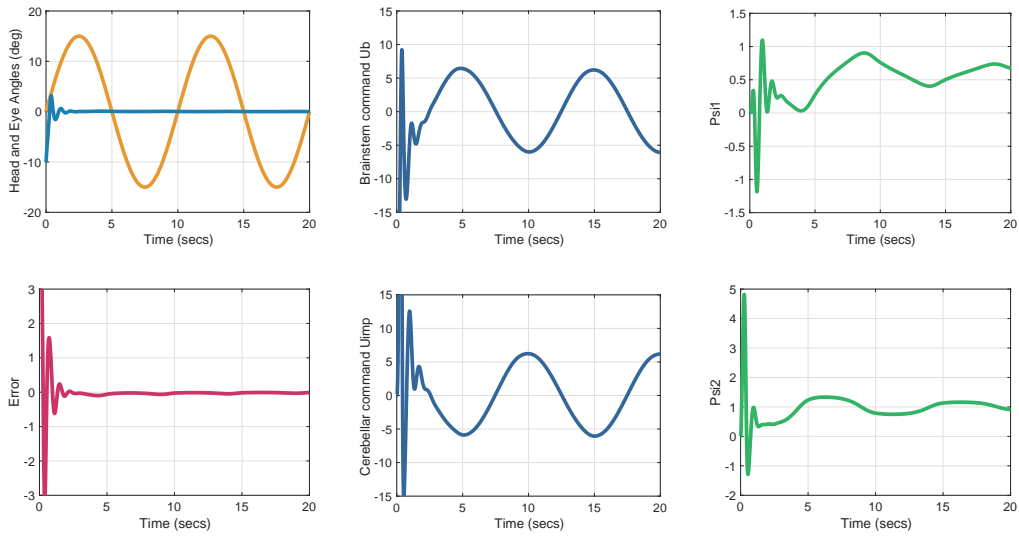


FIGURE 6. VOR cancellation. The signals are the same as in Figure 1.

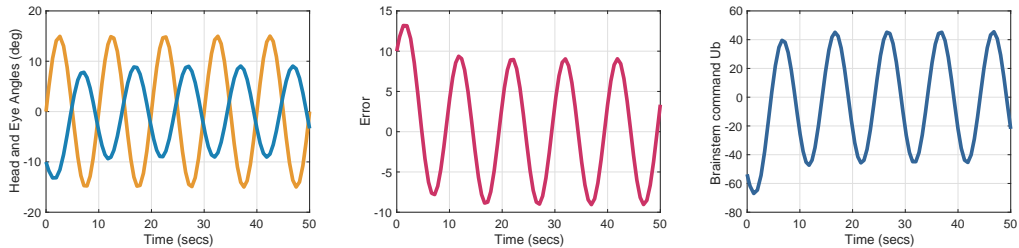


FIGURE 7. VOR cancellation with the cerebellum disabled. From left to right, the head (yellow) and eye (blue) angles, the retinal error e , and the brainstem component u_b .

A careful study of the effects of disabling the neural integrator on the VOR, OKR, gazing holding, and smooth pursuit appeared in [14]. Here we discuss the VOR in the dark. In our model, disabling the neural integrator corresponds to disabling the observer (14a). This means the brainstem component of the control input no longer includes the estimate $-K_x \hat{x}$. Since the VOR is being tested in darkness, the cerebellum makes no compensation for this missing estimate of the oculomotor plant drift term. Therefore, without the

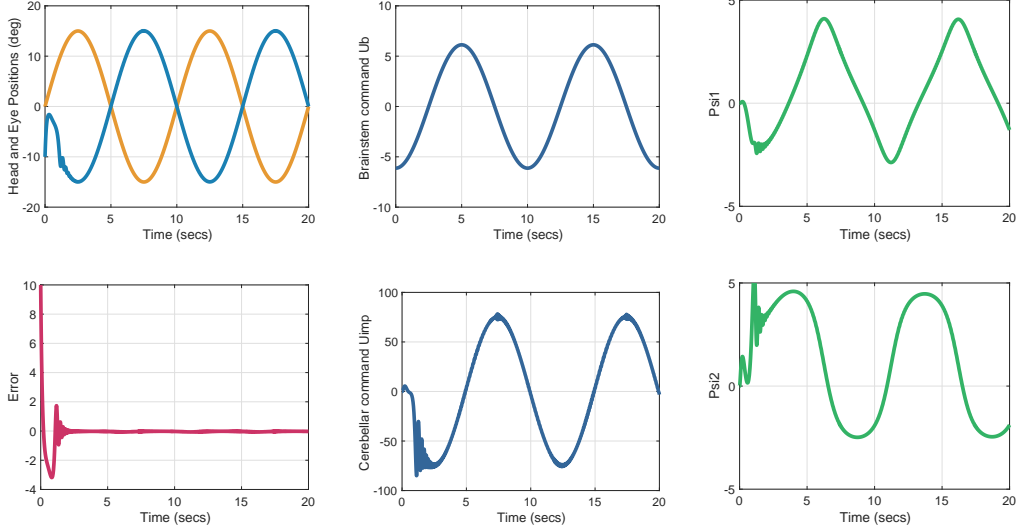


FIGURE 8. VOR in the light with the neural integrator disabled. The signals are the same as in Figure 1.

neural integrator, the eye position evolves according to the dynamics

$$\dot{x} = -K_x x - \alpha_h \dot{x}_h. \quad (16)$$

Comparing with (15), we see the difference is in the constant K_x , which is larger than \tilde{K}_x . For instance, if the head angular velocity is a constant $\dot{x}_h = v$, then eye position converges exponentially to $\bar{x} = -\alpha_h v / K_x$, rather than approximately tracking a ramp (with a very slow exponential decay). This is precisely the behavior recovered in experiments [14]: a step of constant head velocity in total darkness evoked a step change in eye position, not in eye velocity. The author’s of [14] interpreted this behavior by saying “the step in head velocity was not integrated in the brainstem to produce a ramp of eye position”.

A further study of the effects of disabling the neural integrator on the VOR, OKR, and smooth pursuit in monkeys appeared in [33]. They found these systems are minimally affected after a recovery period. Our model predicts that in the light, the cerebellum will compensate for the additional disturbances arising from the removal of the term $-\alpha_x \hat{x}$, such that the VOR is only mildly affected, as reported in [33]. Figure 8 shows the behavior of the VOR in the light with the neural integrator disabled, $x_h(t) = a_h \sin(\beta_h t)$, $a_h = 15$, and $\beta_h = 0.1\text{Hz}$ for $t \in [0, 20]$. We observe the eye moves opposite to the head rotation, as expected.

4.2. OKR. The optokinetic reflex is elicited by movement of large objects in the visual field or movement of the visual surround; it operates in tandem with the VOR. We consider the case of the visual surround rotating sinusoidally, $r_{vs}(t) = -a_v \sin(\beta_v t)$, for example by using an optical drum [1]. The head may be stationary, moving with the visual surround, or moving independently but involuntarily. The eyes may be fixating on a stationary target, a head-fixed target, a drum-fixed target, or a target moving within the moving visual field.

The motion of the visual surround may induce in the subject a perception of a stationary background, with the head and target moving with respect to (w.r.t.) a stationary background. If $r(t)$ and $x_h(t)$ are the target and head angles w.r.t. a fixed inertial frame, then the apparent head and target motion w.r.t. the visual surround are given by $r^{vs}(t) = r(t) - r_{vs}(t)$ and $x_h^{vs}(t) = x_h(t) - r_{vs}(t)$. The perceived error is given by $e = r^{vs} - x_h^{vs} - x = r - x_h - x$. We see that the retinal error is unaffected. Mathematically speaking, the situation is the same as the VOR with a fixed visual surround.

In many experiments with the OKR, the eyes must track a drum-fixed light slit with the head stationary and the optical drum rotating sinusoidally. In this case the error is $e = r - x$, where $r(t) = a_h \sin(\beta_h t)$. We treat this situation as being the same as smooth pursuit, to be discussed below. In an experiment called *OKR cancellation*, a light spot at $r = 0$ is placed in front of a moving striped optical drum. In this case, the pursuit system appears to override the OKR, as the eyes fixate on the fixed light spot, and the error is

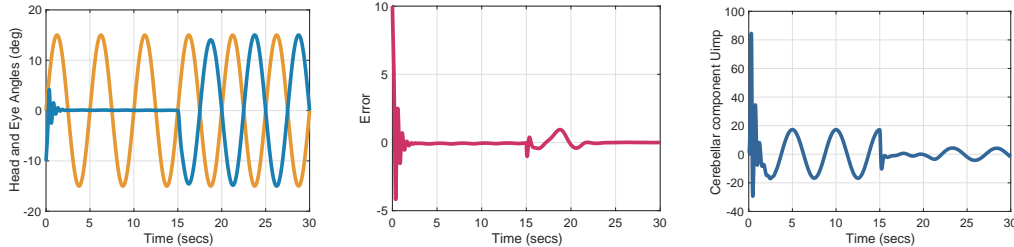


FIGURE 9. Visuo-vestibular conflict in the OKR and its effect on the depth of modulation of the cerebellar output u_{imp} . From left to right, the head (yellow) and eye (blue) angles, the retinal error e , and the cerebellar output u_{imp} .

$e = -x$. If there is no head rotation, then this situation is the same as gaze holding, discussed in the next subsection.

In an experiment called *visual-vestibular conflict* the head and the optokinetic drum are mechanically coupled so that they rotate together, and the eyes must track a light strip on the drum [1]. Therefore, we have $r(t) = x_h(t) = a_h \sin(\beta_h t)$, so $e = r - x_h - x = -x$. From the point of view of our mathematical model, this situation is no different than VOR cancellation. It has been reported that under such stimulation, the modulation of the firing rate of the cerebellum is larger than when the drum is not rotated [72]; that is, when $r(t) = 0$, $x_h(t) = a_h \sin(\beta_h t)$, and $e = -x_h - x$.

In the context of our model, this finding makes sense. In the first case, the role of u_{imp} is to cancel the term $\alpha_h \dot{x}_h$. In the second case, the role of u_{imp} is to cancel the term $-(1 - \alpha_h)\dot{x}_h - \tilde{K}_x x_h$. Assuming that α_h is not close to 0.5 and that \tilde{K}_x is close to zero, the amplitude of the latter term is larger than the amplitude of the former. Figure 9 illustrates this comparison for values $\alpha_h = 0.9$; $a_h = 15$; $\beta_h = 0.2\text{Hz}$; $r = x_h = a_h \sin(\beta_h t)$ for $t \in [0, 15]$; and $r = 0$, $x_h = a_h \sin(\beta_h t)$ for $t \in [15, 30]$.

4.3. Gaze Fixation. Consider the problem of holding the horizontal gaze on a stationary target with an angle $r \neq 0$ while the head is stationary with angle $x_h = 0$. The error is given by $e = r - x$. Assuming that $\hat{x}(t) \simeq x(t)$, the error dynamics (11) take the form

$$\dot{e} = -\tilde{K}_x e - u_c + \tilde{K}_x r. \quad (17)$$

We can see that the role of u_{imp} is to estimate the disturbance $\tilde{K}_x r$. Figure 10 shows the behavior for three target angles: $r(t) = 5^\circ$ for $t \in [0, 15]$; $r(t) = 10^\circ$ for $t \in [15, 30]$, and $r(t) = 15^\circ$ for $t \geq 30$. We observe that the output of the cerebellum is proportional to the eye angle, a behavior observed experimentally in many studies [57]. It arises in our model because u_{imp} must cancel a disturbance $\tilde{K}_x r$, which is proportional to the target position.

Further evidence that $\tilde{K}_x \neq 0$ comes from studies in which the cerebellum is disabled, either through ablation or disease. It is well known that in this case, the eye has a slow drift back to the central position $x = 0$ [15, 57, 62, 69, 82]. For suppose $x_h = 0$ and $u_c = 0$. Then $u = u_b = \alpha_x \hat{x}$, and assuming $\hat{x}(t) \simeq x(t)$, the eye position evolves according to the dynamics

$$\dot{x} = -\tilde{K}_x x.$$

That is, the eye drifts back to center at an exponential rate determined by \tilde{K}_x . Figure 11 depicts this behavior for the same target angles as in Figure 10.

4.4. Smooth Pursuit. We consider a task of the smooth pursuit system in which the eyes must track a horizontally moving target. We assume that any head rotation is involuntary. Let $r(t)$ be the target angle and $x_h(t)$ the head angle. The error is given by $e = r - x_h - x$. Assuming that $\hat{x}(t) \simeq x(t)$, the error dynamics take the general form in (6). We observe that the role of u_{imp} is to estimate the disturbance $\dot{r} + \tilde{K}_x r - (1 - \alpha_h)\dot{x}_h - \tilde{K}_x x_h$.

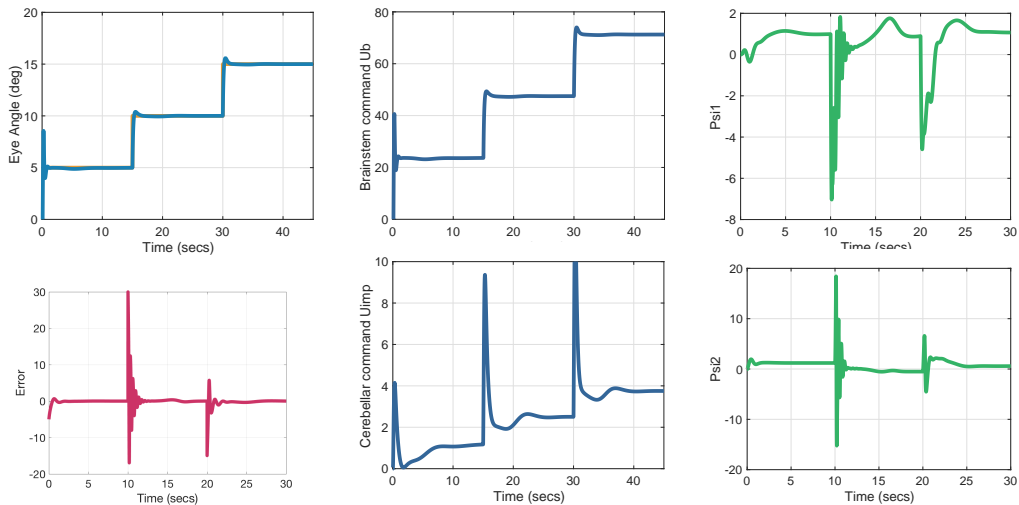


FIGURE 10. Gaze holding. The signals are the same as in Figure 1.

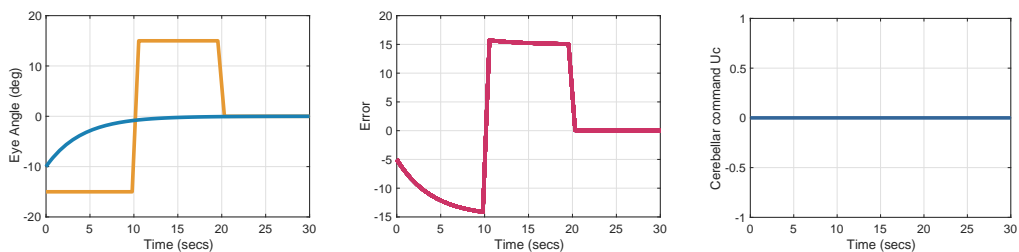


FIGURE 11. Gaze holding with the cerebellum disabled.

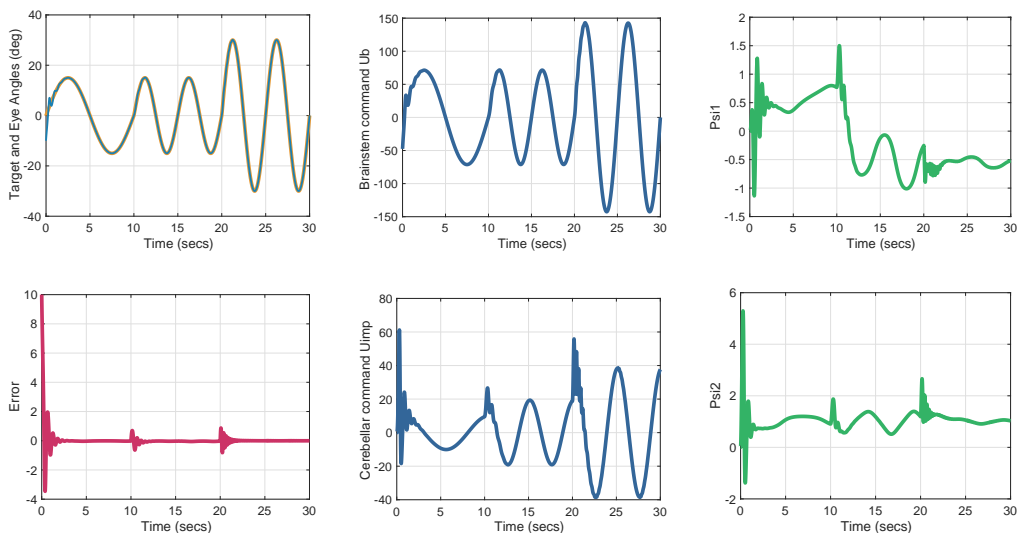


FIGURE 12. Smooth pursuit of a sinusoidal target. The signals are the same as in Figure 1.

Figure 12 depicts smooth pursuit with our model for a sinusoidal target $r(t) = a_h \sin(\beta_h t)$, with $a_h = 15$, $\beta_h = 0.1\text{Hz}$ for $t \in [0, 10]$ and $\beta_h = 0.2\text{Hz}$ for $t \in [10, 20]$. We see that the cerebellar output u_{imp} is strongly modulated during tracking of a sinusoidal target, as observed experimentally [44].

The perfect tracking capability of the smooth pursuit system has been well documented over the years; a small sampling includes [2, 18, 20, 79]. This tracking capability improves as the target motion becomes more predictable [3]. Figure 13 depicts the behavior of our model for smooth pursuit of a target $r(t) =$

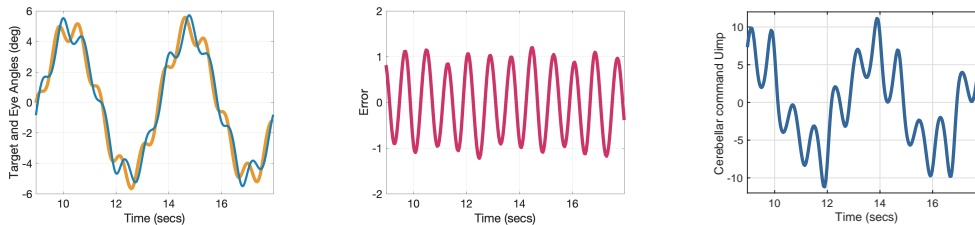


FIGURE 13. Smooth pursuit of a sum of two sinusoids. From left to right, the target angle (yellow) and eye angle (light blue), the error e (red), and the cerebellar output u_{imp} (blue).

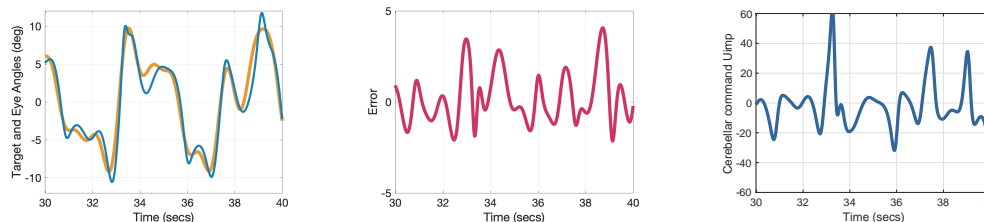


FIGURE 14. Smooth pursuit of a sum of four sinusoids. From left to right, the target angle (yellow) and eye angle (light blue), the error e (red), and the cerebellar output u_{imp} (blue).

$a_1 \sin(2\pi\beta_1 t) + a_2 \sin(2\pi\beta_2 t)$, with $a_1 = 4.85$, $\beta_1 = 0.22\text{Hz}$, $a_2 = 0.853$ and $\beta_2 = 1.25\text{Hz}$. The time interval $t \in [9, 18]$ was chosen to match the data in Figure 1 of [4]. This simulated behavior reproduces what is observed in experiments; namely, that while humans are not capable of perfect tracking of a sum of two or more sinusoids, nevertheless the smooth pursuit system performs reasonably well. The non-zero error displayed in the center of Figure 13 is corroborated by experimental findings in [4].

Figure 14 depicts the behavior of our model for smooth pursuit of a target $r(t) = a_1 \sin(2\pi\beta_1 t) + \dots + a_4 \sin(2\pi\beta_4 t)$, with $a_1 = 6.94$, $\beta_1 = 0.214\text{Hz}$, $a_2 = 2.86$, $\beta_2 = 0.519\text{Hz}$, $a_3 = 2.11$, $\beta_3 = 0.702\text{Hz}$, $a_4 = 1.57$, and $\beta_4 = 0.946\text{Hz}$. The results are comparable to those obtained experimentally as shown in Figure 2 of [18].

It is known that the processing delay for the retinal error to arrive at the cerebellum is on the order of 100ms. Nevertheless, the smooth pursuit system achieves nearly perfect tracking capability; its ability to do so in the face of this delay has been interpreted as a predictive capability [20]. Our model does not impart any prediction to the smooth pursuit system, but the presence of the adaptive internal model aids in overcoming delays. Figure 15 depicts the behavior when tracking a sinusoidal target $r(t) = a \sin(2\pi\beta t)$ with $a = 10$ and $\beta = 0.1\text{Hz}$. The error e has been replaced by $e(t - \tau)$ in (14c) and (14e), with a time delay of $\tau = 107\text{ms}$. The other parameter values are the same as before but we set $K_e = 8$ for closed-loop stability. We observe there is little degradation in the system's tracking capability.

The choice of K_e to achieve closed-loop stability is tied to the time delay and the magnitude of the reference $r(t)$. Figure 16 depicts the largest delay attained with the smallest K_e for varying frequencies and amplitudes of reference signals of the form $r(t) = a \sin(2\pi\beta t)$. With $a = 10$ and $\beta = \{0.1, 0.2\}\text{Hz}$, delays of 107ms and 67ms were achieved with K_e equal to 8 and 13, respectively. Holding $\beta = 0.1\text{Hz}$ but with $a = \{5, 10, 20\}$, the model overcomes delays of 197ms, 107ms, and 56ms with K_e equal to 5, 8 and 15, respectively.

Figure 17 depicts the transient response of our model for smooth pursuit of a ramp target $r(t) = vt$ with $v = 5, 10, 20, 30$. This transient response matches that reported in Figure 3 in [64]. Similar behavior is reported in [78].

In an experiment documented in [43], monkeys were adapted to a new VOR gain by wearing goggles in their cages. It was found that changes in the VOR gain had no effect on the monkey's ability to track a moving target. This behavior is explained in our model when we consider that the cerebellar output u_{imp} compensates for whatever fraction of the vestibular signal entering the error that is not already cancelled by the brainstem component $-\alpha_h \dot{x}_h$.

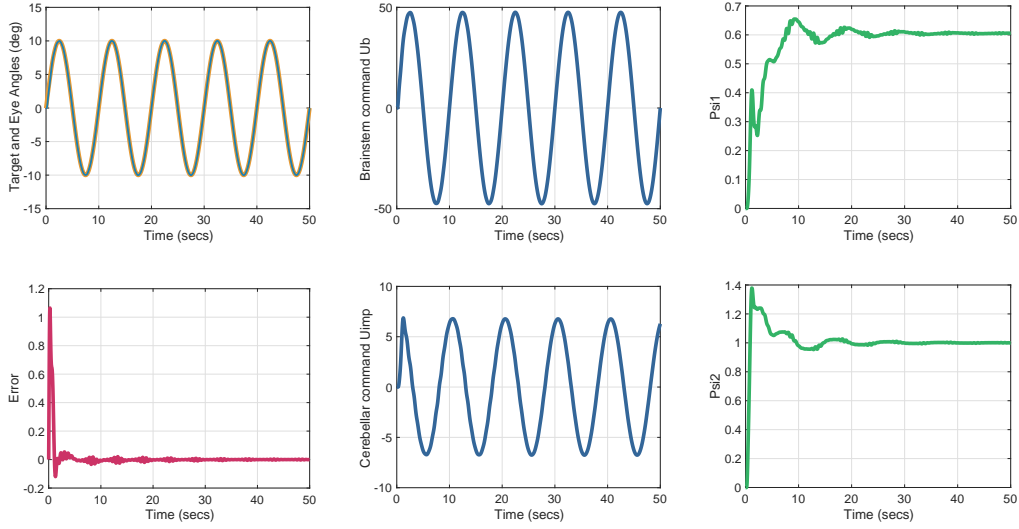


FIGURE 15. Smooth pursuit of a sinusoidal target with a time delay of 107ms in the retinal error signal. The signals are the same as in Figure 1.

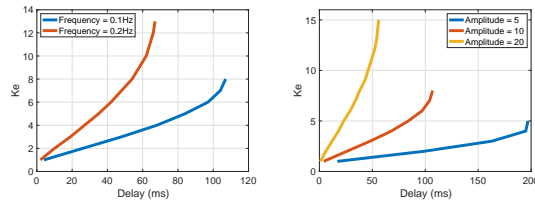


FIGURE 16. Maximum time delay as a function of K_e .

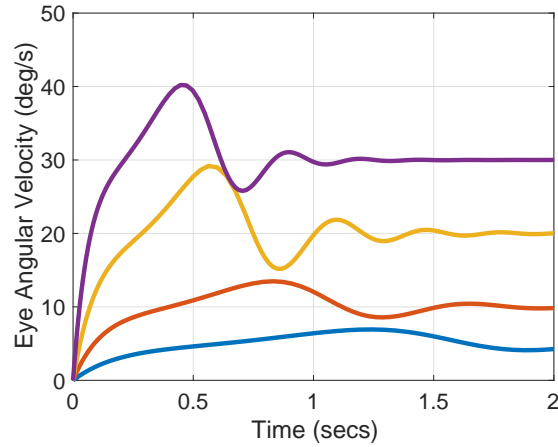


FIGURE 17. Smooth pursuit of a ramp target with velocity $v = 5, 10, 20, 30$ (blue, red, yellow, purple).

The *error clamp* experiment explores the role of the error signal using a technique called *retinal stabilization* [5, 55, 70]. A monkey is trained to track a visual target moving at constant speed. After reaching steady-state, the retinal error is optically clamped at zero using an experimental apparatus that places the target image on the fovea. In experiments it is observed that the eye continues to track the target for some time after. Figure 18 depicts the error clamp behavior with our model, showing that the eye continues to track the target despite the error being clamped at $e \equiv 0$ during the time interval $t \in [5, 6]$.

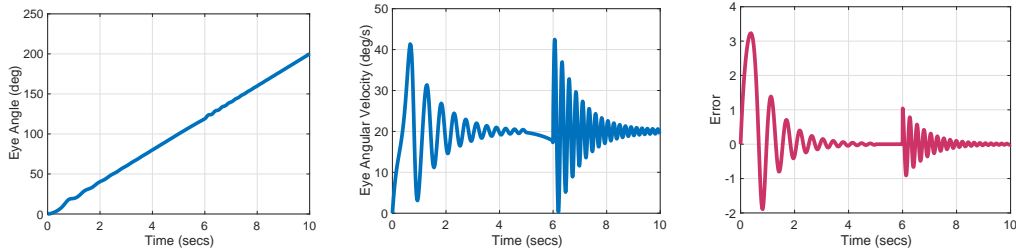


FIGURE 18. Smooth pursuit with an error clamp during $t \in [5, 6]$ s. From left to right, the head angle, the head angular velocity, and the retinal error e .

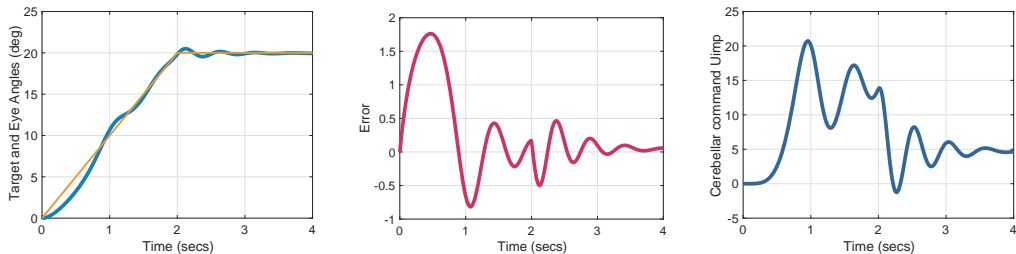


FIGURE 19. Smooth pursuit with target stopping at $t = 2$ s. From left to right, the head angle, the retinal error e , and the cerebellar output u_{imp} .

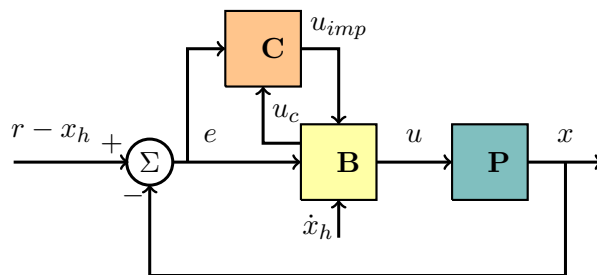


FIGURE 20. Proposed architecture for the oculomotor system. \mathbf{P} is the oculomotor plant, \mathbf{B} is the brainstem, and \mathbf{C} is the cerebellum.

In another series of experiments researchers explored the difference between *target stopping* and *target blanking*. In target stopping, a target with a ramp position is abruptly stopped. It is demonstrated experimentally that during target stopping, the oculomotor system switches from smooth pursuit to gaze holding [40, 42, 64]. In target blanking the target is blanked out or occluded, so that it is no longer visible. It is shown experimentally that with target blanking the eye continues to track for some time [16, 17].

Figure 19 depicts target stopping, in which $r(t) = 10t$ for $t \in [0, 2]$, and $r(t) = 20^\circ$ for $t \geq 2$. We observe that the error decays to zero with an exponential envelope after target stopping, as expected for the gaze holding system. Target blanking may be interpreted in our model as a zero error signal. As we have seen from the results of the error clamp experiment, depicted in Figure 18, the smooth pursuit system continues to track for some time.

5. DISCUSSION

Architecture. Our proposed architecture for the oculomotor system is shown in Figure 20. The symbol \mathbf{P} denotes the oculomotor plant (1); \mathbf{C} is the cerebellum comprising (14b), (14c), and (14e); \mathbf{B} is the brainstem comprising (14a), (14d) and (14f).

An alternative architecture [29, 35] called *feedback error learning* (FEL) is depicted in Figure 21. The primary difference between our architecture and FEL is that in FEL the signals $r, \dot{r}, \ddot{r}, \dots$, which arise from

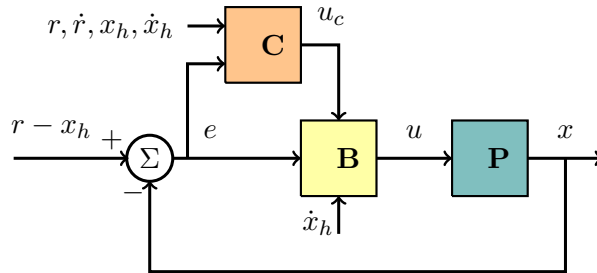


FIGURE 21. Feedback error learning architecture.

exogenous disturbance and reference signals, are assumed to be directly measurable by the cerebellum. These signals are used to estimate model parameters in order to obtain an inverse model of the plant. In contrast, our proposal is that the cerebellum receives only (sensory) error signals, which it uses to reconstruct both persistent, exogenous disturbance and reference signals, as well as model parameters. Indeed, for the oculomotor system, an inverse model is not strictly necessary, since the brainstem neural integrator provides a model of the oculomotor plant. A recent architecture for the computations of the cerebellum emphasizes its role as an adaptive filter [60]. Our model aligns with this interpretation in the sense that we include the standard parameter adaptation law (14c). On the other hand, we explicitly account for the internal model principle, while the architecture in [60] does not.

Limitations. We have already mentioned that we only consider horizontal movement of a single eye. Second, we have not taken explicit account for differences between species. When we cited experimental results for a particular eye movement system, implicitly we restrict to those species that possess such a system. Third, we do not model those signals in the brain that trigger a particular eye movement system; recognizing that trigger signals may be different from driving signals. Fourth, we do not consider detailed models of the semicircular canals of the ear which transmit the vestibular signal, and we do not consider a detailed model of the muscles of the eye. Fifth, we do not consider the role of attention or fatigue of the subject. Sixth, we have not included time delays inherent in the oculomotor system. Finally, we only consider involuntary head movements; voluntary head movements may require a model that bypasses the cerebellum. These modelling omissions were calculated to best illuminate the basic operations of the oculomotor system and the cerebellum.

Open Problems. An important question not directly addressed in our work is: what is the value of q ? We have chosen $q = 2$ based on the fact that disturbance and reference signals are typically steps, ramps, or sinusoids. Additionally, experiments show that humans are able to achieve near perfect tracking of a single sinusoidal reference signal, while tracking the sum of two sinusoids is degraded [79]. Further experimentation is needed to determine the value of q .

A second important question not addressed by our model is long term adaptation (over days and weeks) of system parameters such as the VOR gain. The cerebellum mediates short term adaptation (over the timespan of a single experiment), for instance, by increasing the effective value of the VOR gain to 1. But such short term adaptation is not retained in our model. On the other hand, VOR gain adaptation may be stored in the term α_h in u_b . How is an effective change in VOR gain due to cerebellar *training* transferred to a more permanent change of the parameter α_h in the brainstem? A next step would be to examine the role of persistency of excitation in the parameter adaptation to address this question. Indeed, monkeys deprived of sufficiently rich visual experience following long-term VOR adaptation do not relearn a normal VOR gain [54].

6. CONCLUSION

We have proposed a new model of the oculomotor system, particularly the VOR, OKR, gaze fixation, and smooth pursuit systems. Our key insight is to exploit recent developments on adaptive internal models. Our model recovers behaviors from a number of oculomotor experiments. Additionally, we make a proposal

about the function of the cerebellum: the cerebellum embodies internal models of all persistent, exogenous reference and disturbance signals acting on the body.

REFERENCES

- [1] E. Baarsma and H. Collewijn. Vestibulo-ocular and optokinetic reactions to rotation and their interaction in the rabbit. *J. Physiology*. Vol. 238, pp. 603–625, 1974.
- [2] A.T. Bahill and J. McDonald. Model emulates human smooth pursuit system producing zero-latency target tracking. *Biological Cybernetics*. No. 48, pp. 213-222, 1983.
- [3] A.T. Bahill and J. McDonald. Smooth pursuit eye movements in response to predictable target motions. *Vision Research*. Vo. 23, No. 12, pp. 1573–1583, 1983.
- [4] G.R. Barnes, S.F. Donnelly, and R.D. Eason. Predictive velocity estimation in the pursuit reflex response to pseudo-random and step displacement stimuli in man. *J. Physiology*. Vol. 389, pp. 111-136, 1987.
- [5] G. Barnes, S. Goodbody, and S. Collins. Volitional control of anticipatory ocular pursuit responses under stabilized image conditions in humans. *Experimental Brain Research*. No. 106, pp. 301–317, 1995.
- [6] M. Basso, R. Krauzlis, and R. Wurtz. Activation and inactivation of rostral superior colliculus neurons during smooth-pursuit eye movements in monkeys. *Journal of Neurophysiology*. No. 84, pp. 892–908, 2000.
- [7] A. Berthoz. The role of gaze in compensation of vestibular dysfunction: the gaze substitution hypothesis. *Progress Brain Research*. No. 76, pp. 411-420, 1988.
- [8] G. Blohm, M. Missal, and P. Lefevre. Direct evidence for a position input to the smooth pursuit system. *Journal of Neurophysiology*. Vol. 94, pp. 712-721, 2005.
- [9] M.E. Broucke. Model of the oculomotor system based on adaptive internal models. *IFAC World Congress*. July, 2020.
- [10] M.E. Broucke. Adaptive internal model theory of the oculomotor system and the cerebellum. *IEEE Trans. Automatic Control*. Accepted, November 2020.
- [11] A. Buizza and R. Schmid. Visual-vestibular interaction in the control of eye movement: mathematical modelling and computer simulation. *Biological Cybernetics*. Vol. 43, pp. 209-223, 1982.
- [12] U. Buettner and U. Buttner. Vestibular nuclei activity in the alert monkey during suppression of vestibular and optokinetic nystagmus. *Exp. Brain Res*. No. 37, pp. 581-593, 1979.
- [13] U. Buttner and W. Waespe. Purkinje cell activity in the primate flocculus during optokinetic stimulation, smooth pursuit eye movements, and VOR-suppression. *Exp. Brain Res*. No. 55, pp. 97-104, 1984.
- [14] S. Cannon and D. Robinson. Loss of the neural integrator of the oculomotor system from brain stem lesions in monkey. *J. Neurophysiology*. Vol. 57, No. 5, pp. 1383-1409, May 1987.
- [15] R.H.S. Carpenter. Cerebellectomy and the transfer function of the vestibulo-ocular reflex in the decerebrate cat. *Proc. Royal Society of London. Series B, Biological Sciences*. Vol. 181, No. 1065, pp. 353–374, July 1972.
- [16] N. Cerminara, R. Apps, and D. Marple-Horvat. An internal model of a moving visual target in the lateral cerebellum. *J. Physiology*. vol. 587, no. 2, pp. 429-442, 2009
- [17] M. Churchland, I. Chou, and S. Lisberger. Evidence for object permanence in the smooth-pursuit eye movements of monkeys. *J. Neurophysiology*. No. 90, pp. 2205-2218, 2003.
- [18] H. Collewijn and E. Tamminga. Human smooth and saccadic eye movements during voluntary pursuit of different target motions on different backgrounds. *J. Physiology*. vol. 351, pp. 217-250, 1984.
- [19] A. Dale and K. Cullen. Local population synchrony and the encoding of eye position in the primate neural integrator. *J. Neuroscience*. Vol. 35, No. 10, pp. 4287-4295, March 2015.
- [20] D.C. Deno, W.F. Crandall, K. Sherman, E. Keller. Characterization of prediction in the primate visual smooth pursuit system. *BioSystems*. vol. 34, pp. 107–128, 1995.
- [21] S. Eggers, N. de Pennington, M. Walker, M. Shelhamer, and D. Zee. Short-term adaptation of the VOR: non-retinal-slip error signals and saccade substitution. *Ann. N.Y. Academy of Sciences*. No. 1004, pp. 94-110, 2003.
- [22] B.A. Francis. The linear multivariable regulator problem. *SIAM J. Control and Optimization*. Vol. 15, No. 3, pp. 486–505, May 1977.
- [23] B.A. Francis and W.M. Wonham. The internal model principle for linear multivariable regulators. *Applied Mathematics and Optimization*. Vol. 2, No. 2, 1975.
- [24] B.A. Francis and W.M. Wonham. The internal model principle of control theory. *Automatica*. Vol. 12, pp. 457–465, 1976.
- [25] J. Eccles, M. Ito, and J. Szentagothai. *The Cerebellum as a Neuronal Machine*. Springer-Verlag, 1967.
- [26] H. Galiana and J. Outerbridge. A bilateral model for central neural pathways in vestibuloocular reflex. *Journal of Neurophysiology*. Vol. 51, no. 2, pp. 210–241, February 1984.
- [27] N.M. Gerrits, A.H. Epema, A. van Linge, and E. Dalm. The primary vestibulocerebellar projection in the rabbit: absence of primary afferents in the flocculus. *Neuroscience Letters*. Vol. 105, pp. 27-33, 1989.
- [28] S. Glasauer. Cerebellar contribution to saccades and gaze holding. *Annals New York Academy of Sciences*. pp. 206-209, 2003.
- [29] H. Gomi and M. Kawato. Adaptive feedback control models of the vestibulocerebellum and spinocerebellum. *Biological Cybernetics*. Vol. 68, pp. 105-114, 1992.

- [30] A. Green, Y. Hirata, H. Galiana, and S. Highstein. Localizing sites for plasticity in the vestibular system. In: Highstein S.M., Fay R.R., Popper A.N. (eds) *The Vestibular System*. Vol. 19. Springer, 2004.
- [31] A. Green, H. Meng, and D. Angelaki. A reevaluation of the inverse dynamic model for eye movements. *Journal of Neuroscience*. Vol. 27, no. 6, pp. 1346–1355, February, 2007.
- [32] B. Guthrie, J. Porter, and D. Sparks. Corollary discharge provides accurate eye position information to the oculomotor system. *Science*. Vol. 221, pp. 1193-1195, September 1983.
- [33] C.R. Kaneko. Eye movement deficits after ibotenic acid lesions of the nucleus prepositus hypoglossi in monkeys, II: Pursuit, vestibular, and optokinetic responses. *J. Neurophysiology*. Vol. 81, pp. 668 - 681, 1999.
- [34] M. Kawato. Internal models for motor control and trajectory planning. *Current Opinion in Neurobiology*. Vol. 9, No. 6, pp. 718-727, December 1999.
- [35] M. Kawato and H. Gomi. A computational model of four regions of the cerebellum based on feedback-error learning. *Biological Cybernetics*. Vol. 68, pp. 95-103, 1992.
- [36] E. Keller and P. Daniels. Oculomotor related interaction of vestibular nucleus cells in alert monkey. *Exp. Neurology*. No. 46, pp. 187-198, 1975.
- [37] E. L. Keller and D. A. Robinson. Absence of a stretch reflex in extraocular muscles of the monkey. *Journal of Neurophysiology*. Vol. 34, No. 5, pp. 908-919, September 1971.
- [38] R. Krauzlis. Recasting the smooth pursuit eye movement system. *J. Neurophysiology*. No. 91, pp. 591-603, 2004.
- [39] R. Krauzlis, M. Basso, and R. Wurtz. Shared motor error for multiple eye movements. *Science*. No. 276, pp. 1693–1695, 1997.
- [40] R. Krauzlis and F. Miles. Transitions between pursuit eye movements and fixation in the monkey: dependence on context. *J. Neurophysiology*. No. 76, pp 1622-1638, 1996.
- [41] S. Lisberger and A. Fuchs. Role of primate flocculus during rapid behavioral modification of vestibular reflex I: Purkinje cell activity during visually guided horizontal smooth-pursuit eye movements and passive head rotation. *J. Neurophysiology*. Vol. 41, no. 3, May 1978.
- [42] A. Luebke and D. Robinson. Transition dynamics between pursuit and fixation suggest different systems. *Vision Research*. Vol. 28, No. 8, pp. 941-946, 1988.
- [43] S. Lisberger. Neural basis for motor learning in the vestibuloocular reflex of primates. III. Computational and behavioral analysis of the sites of learning. *J. Neurophysiology*. Vol. 72, No. 2, August 1994.
- [44] S. Lisberger. Internal models of eye movement in the floccular complex of the monkey cerebellum. *Neuroscience*. Vol. 162, No. 3, pp. 763–776, September, 2009.
- [45] S. Lisberger. Visual guidance of smooth pursuit eye movements. *Annual Rev. Vis. Sci.* No. 1, pp. 447-468, 2015.
- [46] S. Lisberger and A. Fuchs. Role of primate flocculus during rapid behavioral modification of vestibuloocular reflex. I. Purkinje cell activity during visually guided horizontal smooth-pursuit eye movements and passive head rotation. *J. Neurophysiology*. Vol. 41, no. 3, pp. 733–763, May 1978.
- [47] S. Lisberger and T. Pavelko. Vestibular signals carried by pathways subserving plasticity of the vestibulo-ocular reflex in monkeys. *Journal of Neuroscience*. No. 6, Vol. 2, pp. 346-354, February 1986.
- [48] G. Mandl, G. Melvill Jones, and M. Cynader. Adaptability of the vestibulo-ocular reflex to vision reversal in strobe reared cats. *Brain Research*. Vol. 209, No. 1, pp. 35-45, 1981.
- [49] R. Marino and P. Tomei. An adaptive learning regulator for uncertain minimum phase systems with undermodeled unknown exosystems. *Automatica*. No. 47, pp. 739–747, 2011.
- [50] G. Melvill Jones and G. Mandl. Effects of strobe light on adaptation of vestibulo-ocular reflex (VOR) to vision reversal. *Brain Research*. No. 164, pp. 300-303, 1979.
- [51] R.C. Miall and D.M. Wolpert. Forward models for physiological motor control. *Neural Networks*. Vol. 9, No. 8, pp. 1265–1279, 1996.
- [52] J.A. Michael and G. Jones. Dependence of visual tracking capability upon stimulus predictability. *Vision Research*. Vol. 6, Issue 11-12, pp. 707-716, 1966.
- [53] F. Miles and B. Eighmy. Long-term adaptive changes in primate vestibuloocular reflex. I. Behavioral observations. *J. Neurophysiology*. Vol. 43, No. 5, May 1980.
- [54] F. Miles and J. H. Fuller. Adaptive plasticity in the vestibulo-ocular responses of the rhesus monkey. *Brain Research*. Vol. 80, pp. 512-516, 1974.
- [55] E. Morris and S. Lisberger. Different responses to small visual errors during initiation and maintenance of smooth-pursuit eye movements in monkeys. *J. Neurophysiology*. Vol. 58, no. 6, pp. 1351-1369, 1987.
- [56] V.O. Nikiforov. Adaptive non-linear tracking with complete compensation of unknown disturbances. *European Journal of Control*. Vol. 4, pp. 132–139, 1998.
- [57] H. Noda and D. Suzuki. The role of the flocculus of the monkey in fixation and smooth pursuit eye movements. *J Physiology*. No. 294, pp. 335–348, 1979.
- [58] J. Pola. Models of the saccadic and smooth pursuit systems. In: G. Hung, K. Ciuffreda (eds). *Models of the Visual System*. Springer, 2002.
- [59] J. Pola and H. Wyatt. Target position and velocity: the stimulus for smooth pursuit eye movement. *Vision Research*. No. 20, pp. 523-534, 1980.

- [60] J. Porrill, P. Dean, and J. Stone. Recurrent cerebellar architecture solves the motor-error problem. *Proc. Royal Soc. Lond. B.* No. 271, pp. 789-796, 2004.
- [61] D. A. Robinson. Oculomotor unit behavior in the monkey. *J. Neurophysiology.* No. 33, pp. 393-404. 1970.
- [62] D. A. Robinson. The effect of cerebellectomy on the cat's vestibulo-ocular integrator. *Brain Research.* Vol. 71, pp. 195-207, 1974.
- [63] D.A. Robinson. The use of control systems analysis in the neurophysiology of eye movements. *Ann. Rev. Neuroscience.* No. 4, pp. 463-503, 1981.
- [64] D.A. Robinson, J.L. Gordon, and S.E. Gordon. A model of the smooth pursuit eye movement system. *Biological Cybernetics.* No. 55, pp. 43-57, 1986.
- [65] A. Serrani and A. Isidori. Semiglobal nonlinear output regulation with adaptive internal model. *IEEE Conference on Decision and Control.* pp. 1649-1654, December, 2000.
- [66] A. Serrani, A. Isidori, L. Marconi. Semiglobal nonlinear output regulation with adaptive internal model. *IEEE Transactions on Automatic Control.* Vol. 46, No. 8, pp. 1178-1194, 2001.
- [67] M. Shelhamer, B. Ravina, and P. Kramer. Adaptation of the gain of the angular vestibulo-ocular reflex when retinal slip is zero. *Soc. Neuroscience Abstracts.* No. 21, p. 518, 1995.
- [68] M. Shelhamer, C. Tiliket, and D. Roberts, et al. Short-term vestibulo-ocular reflex adaptation in humans II. Error signals. *Experimental Brain Research.* No. 100, pp. 328-336, 1994.
- [69] A. Skavenski and D. Robinson. Role of abducens neurons in vestibuloocular reflex. *J. Neurophysiology.* No. 36, pp. 724-738, 1973.
- [70] L. Stone and S. Lisberger. Visual responses of purkinje cells in the cerebellar flocculus during smooth-pursuit eye movements in monkeys I. simple spikes. *Journal of Neurophysiology.* Vol. 63, No. 5, pp. 1241-1261, May 1990.
- [71] P. Sylvestre and K. E. Cullen. Quantitative analysis of abducens neuron discharge dynamics during saccadic and slow eye movements. *Journal of Neurophysiology.* Vol. 82, issue 5, pp. 2612-2632, November 1999.
- [72] W. Waespe and V. Henn. Conflicting visual-vestibular stimulation and vestibular nucleus activity in alert monkeys. *Experimental Brain Research.* Vol. 33, pp. 203-211, 1978.
- [73] D. Wolpert, Z. Ghahramani, and M. Jordan. An internal model for sensorimotor integration. *Science,* Vol. 269, No. 5232, pp. 1880-1882, September 1995.
- [74] D. Wolpert and M. Kawato. Multiple paired forward and inverse models for motor control. *Neural Networks.* Vol. 11, pp. 1317-1329, 1998.
- [75] D. Wolpert, R.C. Miall, and M. Kawato. Internal models in the cerebellum. *Trends in Cognitive Sciences.* Vol. 2, no. 9, pp. 338-347, September 1998.
- [76] H. Wyatt and J. Pola. Slow eye movements to eccentric targets. *Investigative Ophthalmology and Visual Science.* No. 21, pp. 477-483, 1981.
- [77] H. Wyatt and J. Pola. Smooth pursuit eye movements under open-loop and closed-loop conditions. *Vision Research.* Vol. 23, No. 10, pp. 1121-1131, 1983.
- [78] H.J. Wyatt and J. Pola. Smooth eye movements with step-ramp stimuli: the influence of attention and stimulus extent. *Vision Research.* 27, pp. 1121-1131, 1983.
- [79] H.J. Wyatt and J. Pola. Predictive behavior of optokinetic eye movements. *Exp. Brain Res.* No. 73, pp. 615-626, 1988.
- [80] S. Yasui and L.R. Young. Perceived visual motion as effective stimulus to pursuit eye movement system. *Science.* No. 190, pp. 906-908, 1975.
- [81] L.R. Young and L. Stark. Variable feedback experiments testing a sampled data model for eye tracking movements. *IEEE Trans. Human Factors in Electronics.* No. 4, pp. 38-51, 1963.
- [82] D. Zee, R. Yee, D. Cogan, D. Robinson, and W. Engel. Ocular motor abnormalities in hereditary cerebellar ataxia. *Brain.* No. 99, pp. 207-234, 1976.
- [83] D. Zee, A. Yamazaki, P. Butler, and G. Gucer. Effects of ablation of flocculus and paraflocculus on eye movements in primate. *J. Neurophysiology.* Vol. 46, No. 4, pp. 878-899, October 1981.
- [84] X. Zhang and H. Wakamatsu. A unified adaptive oculomotor control model. *International Journal of Adaptive Control and Signal Processing.* No. 15, pp. 697-713, 2001.
- [85] W. Zhou, P. Weldon, B Tang and W. King. Retinal slip is not required for rapid adaptation of the translational vestibulo-ocular reflex. *Soc. Neuroscience Abstracts.* No. 27, 2001.

APPENDIX A.

In this section we prove that the controller (14) solves Problem 3.1; the proof closely mimicks that of [65]. First we state the result for transforming the exosystem (7) into the form (10).

Lemma A.1 ([56]). *Let $F \in \mathbb{R}^{q \times q}$ and $G \in \mathbb{R}^q$. Suppose that (F, G) is a controllable pair and (E, S) is an observable pair. Also suppose that F is Hurwitz, and F and S have disjoint spectra. Then the Sylvester equation*

$$MS = FM + GE \tag{18}$$

has a unique solution $M \in \mathbb{R}^{q \times q}$ which is nonsingular.

Consider the error dynamics in (11) and the estimation error $\tilde{x} = x - \hat{x}$. If we take the states of the closed-loop system to be $(e, \hat{w}, \tilde{x}, \hat{\Psi})$, then the closed-loop system is

$$\dot{e} = -(\tilde{K}_x + K_e)e + \alpha_x \tilde{x} - \hat{\Psi} \hat{w} + \Psi w \quad (19a)$$

$$\dot{\hat{w}} = (F + G\hat{\Psi})\hat{w} + GK_e e \quad (19b)$$

$$\dot{\tilde{x}} = -K_x \tilde{x} \quad (19c)$$

$$\dot{\hat{\Psi}} = e \hat{w}^T, \quad (19d)$$

Define the exosystem and parameter estimation errors: $\tilde{w} := \hat{w} - w + Ge$ and $\tilde{\Psi} := \hat{\Psi} - \Psi$. In terms of these errors we have

$$\dot{e} = -Ke + \alpha_x \tilde{x} - \Psi \tilde{w} - \tilde{\Psi} \hat{w} \quad (20a)$$

$$\dot{\tilde{w}} = F\tilde{w} - He + \alpha_x G\tilde{x} \quad (20b)$$

$$\dot{\tilde{x}} = -K_x \tilde{x}, \quad (20c)$$

where $K := K_x - \alpha_x + K_e - \Psi G$ and $H := FG + G\tilde{K}_x$. Suppose that $\tilde{\Psi} = 0$ in (20), and let $\tilde{\xi} := (\tilde{w}, \tilde{x})$. Then (20) becomes

$$\dot{e} = -Ke + \tilde{G}\tilde{\xi} \quad (21a)$$

$$\dot{\tilde{\xi}} = \tilde{F}\tilde{\xi} + \tilde{H}e \quad (21b)$$

where $\tilde{F} = \begin{bmatrix} F & \alpha_x G \\ 0 & -K_x \end{bmatrix}$, $\tilde{G} = [-\Psi \quad \alpha_x]$, and $\tilde{H} = \begin{bmatrix} -H \\ 0 \end{bmatrix}$. By assumption F is Hurwitz and $K_x > 0$, so \tilde{F} is Hurwitz. Given any $\gamma > 0$, there exists a symmetric, positive definite matrix $P \in \mathbb{R}^{(q+1) \times (q+1)}$ such that $P\tilde{F} + \tilde{F}^T P = -\gamma I$. Define the Lyapunov function for the system (21):

$$V := \|e\|^2 + \tilde{\xi}^T P \tilde{\xi}.$$

Then along solutions of (21), we have

$$\begin{aligned} \dot{V} &= -2K\|e\|^2 + 2e\tilde{G}\tilde{\xi} + 2\tilde{\xi}^T P \tilde{H}e - \gamma\|\tilde{\xi}\|^2 \\ &= \begin{bmatrix} e^T & \tilde{\xi}^T \end{bmatrix} \begin{bmatrix} -2K & \tilde{H}^T P + \tilde{G} \\ P\tilde{H} + \tilde{G}^T & -\gamma I \end{bmatrix} \begin{bmatrix} e \\ \tilde{\xi} \end{bmatrix} \\ &=: \begin{bmatrix} e^T & \tilde{\xi}^T \end{bmatrix} \tilde{Q} \begin{bmatrix} e \\ \tilde{\xi} \end{bmatrix}. \end{aligned}$$

Since the unknown parameters (\tilde{K}_x, Ψ^T) belong to a compact set \mathcal{P} , the off-diagonal elements of \tilde{Q} are bounded. Then by a standard argument we can choose $K > 0$ sufficiently large (by choosing $K_e > 0$ sufficiently large) such that \tilde{Q} is negative definite for all $(\tilde{K}_x, \Psi^T) \in \mathcal{P}$.

Now consider (20) with $\tilde{\Psi} \neq 0$ and define the Lyapunov function

$$V_\Psi := V + \tilde{\Psi} \tilde{\Psi}^T.$$

Let $\dot{V}_{(21)}$ denote the Lie derivative of V along solutions of (21) (with $\tilde{\Psi} = 0$). Evaluating the derivative of V_Ψ along solutions of (20) and invoking (19d), we obtain

$$\dot{V}_\Psi = \dot{V}_{(21)} - 2e\tilde{\Psi}\hat{w} + 2\tilde{\Psi}\dot{\hat{\Psi}}^T = \dot{V}_{(21)},$$

which is again negative definite at $(e, \tilde{w}, \tilde{x}) = (0, 0, 0)$. Finally, applying the LaSalle Invariance Principle, we obtain that $\lim_{t \rightarrow \infty} e(t) = 0$, as required.